



Giant Self-biased Magnetoelectric Effect in Pre-biased Magnetostrictive–Piezoelectric Laminate Composites

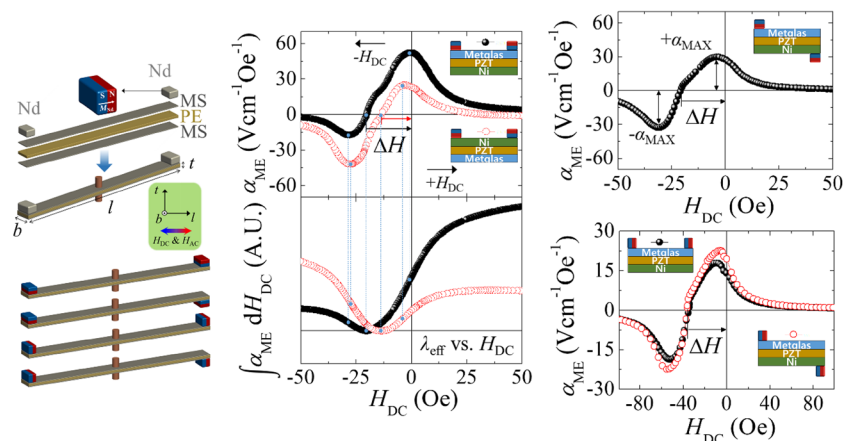
Yong-Woo Lee¹ · Bipul Deka^{1,2} · Il-Ryeol Yoo¹ · Do-Woo Gwak¹ · Jiung Cho³ · Hyun-Cheol Song⁴ · Jong-Jin Choi⁵ · Byung-Dong Hahn⁵ · Cheol-Woo Ahn⁵ · Kyung-Hoon Cho^{1,2}

Received: 30 October 2019 / Accepted: 2 December 2019 / Published online: 17 December 2019
© The Korean Institute of Metals and Materials 2019

Abstract

In this study, it is demonstrated that the giant self-biased magnetoelectric (SME) response can be achieved from a center-clamped magnetostrictive–piezoelectric laminate composite by employing magnetic tip masses. An asymmetric laminate structure consisting of two different magnetostrictive layers (Metglas and nickel) with opposite signs of piezomagnetic coefficient is introduced to promote structural bending resonance, and the effect of layout change of attaching the magnetic tip masses on SME responses is systematically investigated. The highest SME effect is observed when all magnetic tip masses are loaded on the Metglas layer and their magnetization directions are normal to the Metglas surface. It is proposed that not only the parallel magnetic domains to external magnetic field but also the non-parallel magnetic domains effectively contribute to the total magnetostriction. The fabricated SME laminates exhibit giant SME voltage coefficients ranging from 14.11 to 52.35 V cm⁻¹ Oe⁻¹, depending on the direction of the fields of the tip magnets. These high SME voltage output values and their controllability are promising for precision field sensors, magnetic energy harvesters and field-tunable devices.

Graphic Abstract



Keywords Self-biased · Magnetoelectric · Composite · Magnetostriction

✉ Jiung Cho
jiung14@kbsi.re.kr

✉ Cheol-Woo Ahn
cheoruahn@kims.re.kr

✉ Kyung-Hoon Cho
khcho@kumoh.ac.kr

¹ School of Materials Science and Engineering, Kumoh National Institute of Technology, Gumi 39177, Republic of Korea

² Advanced Materials Research Center, Kumoh National Institute of Technology, Gumi 39177, Republic of Korea

³ Western Seoul Center, Korea Basic Science Institute, Seoul 03579, Republic of Korea

⁴ Center for Electronic Materials, Korea Institute of Science and Technology, Seoul 02792, Republic of Korea

⁵ Korea Institute of Materials Science (KIMS), Changwon 51508, Republic of Korea

1 Introduction

Multiferroic magnetoelectric (ME) composites consisting of piezoelectric (PE) and magnetostrictive (MS) materials pave new dimensions in various technologies including magnetic sensors, voltage tunable inductors, data storage elements, spintronic, energy harvesters, etc. [1–3]. The ME effect in ME composites is a product property of the PE and MS phases through their interfacial coupling [4, 5]. The transfer of mechanical strain between the two phases induces a change in electric polarization in the PE phase or magnetic flux in the MS phase, and the effect is known to be the largest in 2–2 laminate structures [1, 6–8]. Since the strain in the MS phase, which determines the overall performance of the ME device, follows a quadrature dependence of DC bias magnetic field (H_{DC}), an external H_{DC} is essential to elicit the best ME performance. The requirement of an external H_{DC} imposes several concerns of the device including electromagnetic interference and system bulkiness as well [3].

In order to circumvent the limitations caused by the necessity of an external H_{DC} , self-biased ME composites have been investigated extensively in recent years [9]. Self-biased magnetoelectric (SME) effect is defined as the ME coupling under an external AC magnetic field (H_{AC}) when $H_{DC} = 0$. There are five main types of SME composites that have been investigated both experimentally and theoretically: (a) functionally graded ferromagnetic (FM)-based SME; (b) exchange bias-mediated SME; (c) magnetostriction hysteresis-based SME; (d) built-in stress-mediated SME and (e) non-linear SME [4, 9]. Exchange biasing of MS layer is found to be one of the most promising way to achieve SME [4, 10]. Exchange bias (EB) refers to the shift of magnetic hysteresis ($M-H$) loop along the field axis, and it is commonly observed in magnetic materials containing hard and soft magnetic phases when cooled through the Néel temperature of antiferromagnetic phase under a suitable magnetic field [4, 10–12]. The magnetization shift of the FM layer in laminate composites due to EB field yields corresponding shift in magnetostriction (λ) versus H_{DC} curve of the FM layer, resulting in SME response [9]. Most of the previous studies of EB-mediated SME effects in ME composites have focused on the EB controlled by an external electric field (converse ME effect) [13, 14]. The magnetically controlled EB-mediated SME effect is very rarely reported, although it is important in direct ME devices such as sensors, tunable transformers and energy harvesters [10, 14]. The lack of progress in EB-mediated SME response is due to the difficulties in synthesizing heterogeneous FM materials, requirements of the special protocol including field-cooling, degradation of EB over time, reciprocal dependences on magnetostrictive layer thickness, etc.

Similar to the EB-mediated approach, but much simpler, a pre-applied magnetic field inside the MS layer can be implemented by employing permanent magnets to shift λ versus H_{DC} curve. This approach is expected to be applied to any desired MS materials without complicated experimental procedures. More importantly, deterioration of device characteristics over time is not expected because “permanent” magnet is utilized. Nevertheless, no systematic studies have yet been conducted to verify this method and to understand underlying physical mechanism. Here, we report giant SME effects in MS/PE/MS laminate composite, clamped at its nodal point, with its free ends loaded with magnetic tip masses. Four different layouts of attaching the magnetic tip masses were explored to derive the optimal structure to secure high SME performance. A very high SME voltage coefficient of $52.35 \text{ V cm}^{-1} \text{ Oe}^{-1}$ was achieved from the simple laminate structure. To understand the mechanism behind the giant SME response, we discuss the correlation between tendencies of ME voltage versus H_{DC} curve, distribution of pre-applied magnetic field and resultant magnetization of MS layer.

2 Results and Discussion

Figure 1a shows the design schematics of the laminate composite composed of a PE layer sandwiched between two MS layers. The laminate is clamped at its center (nodal point), and its free ends are loaded with a pair of NdFeB (Nd) permanent magnets as tip masses. The magnetic fields of the two Nd magnets can be combined to form a pre-applied magnetic field (H_{PA}) in the MS layers along the longitudinal direction of the laminate. To induce the H_{PA} collinear to H_{DC} through the MS layers, we considered four layouts of attaching Nd magnets as shown in Fig. 1b: (i) the direction of magnetization of Nd magnets (\overline{M}_{Nd}) is perpendicular to the longitudinal direction of the laminate ($\overline{M}_{Nd}(\perp)$ case) and Nd magnets are attached to only one MS layer; (ii) \overline{M}_{Nd} is perpendicular to the longitudinal direction of the laminate and Nd magnets are attached to both MS layers; (iii) \overline{M}_{Nd} is parallel to the longitudinal direction of the laminate ($\overline{M}_{Nd}(\parallel)$ case) and Nd magnets are attached to only one MS layer; (iv) \overline{M}_{Nd} is parallel to the longitudinal direction of the laminate and Nd magnets are attached to both MS layers. The four layouts in Fig. 1b are all intended to form H_{PA} inside the MS layers by attractive magnetic force between two Nd magnets. Note that any repulsive configuration of Nd magnets was found to be ineffective for the SME response (i.e., for the shift of λ vs. H_{DC} curve).

To fabricate the laminate composites, two different MS materials, FeSiB-based alloy (Metglas, stacked to 150 μm -thick, 2605SA1, Metglas Inc.) and nickel (Ni, 160 μm -thick, 99+%, Nilaco Corp.), were used as upper

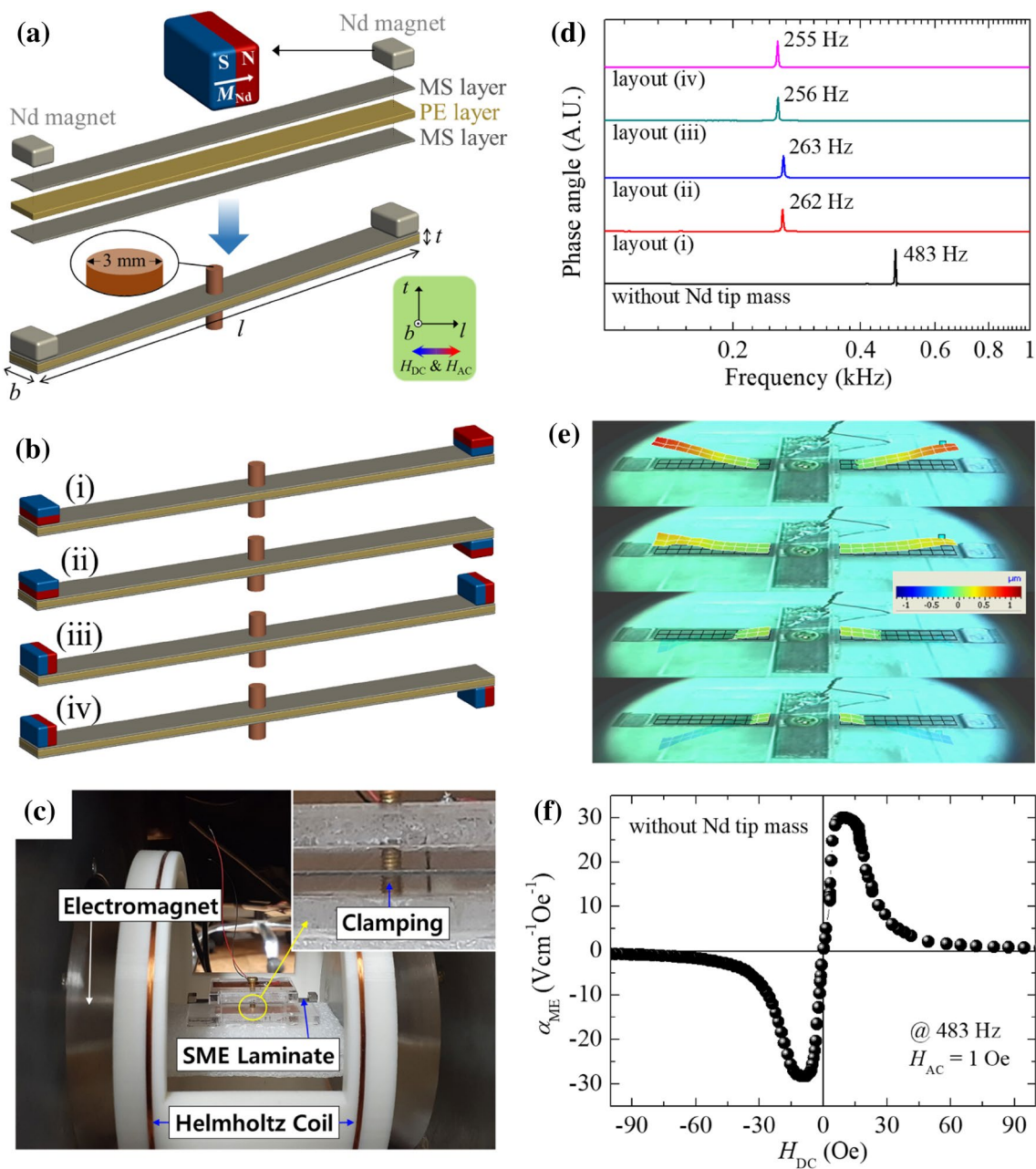


Fig. 1 **a** Design schematics of self-biased magnetoelastic laminate composed of two magnetostrictive layers, one piezoelectric layer and two Nd magnets. **b** Various layouts of attaching Nd magnets at the free ends of the laminate. **c** Photograph of equipment for measuring magnetoelastic voltage output from the laminate. **d** Phase angle

spectra of Metglas/PZT/Ni laminates with the layouts represented in **b**. **e** Bending motion images of Metglas/PZT/Ni laminate with layout (i) in **b** measured under 2 V at 262 Hz. **f** α_{ME} versus H_{DC} curve of Metglas/PZT/Ni laminate without Nd tip mass. (Color figure online)

and lower MS layers. As a PE material, $\text{Pb}(\text{Zr}, \text{Ti})\text{O}_3$ (PZT)-based 31-mode piezoelectric ceramics (250 μm -thick, PSI-5H4E, Piezo Systems Inc.) poled along the thickness direction was used. The Metglas and Ni were attached to the top and bottom surfaces of the PZT layer by using epoxy adhesive (DP460, 3 M) and cured at 80 $^{\circ}\text{C}$. Areal dimensions of all constitutive layers were fixed at 60 mm (l) \times 5 mm (b). Then, two small Nd magnets (6 mm \times 4 mm \times 3 mm) were

attached to end surfaces of the MS layers to complete the laminate structures in Fig. 1b. The phase angle spectra of the laminates was measured by using an impedance analyzer (IM3570, Hioki). The actuation shape of the laminate was visualized using a scanning laser vibrometer (Polytec, PSV 500). To characterize ME responses, the laminate was placed at the center of a Helmholtz coil located at the center of the electromagnet (Fig. 1c), and the voltage induced on the

laminated was monitored using a lock-in amplifier (SR860, Stanford Research System).

Since the sign of piezomagnetic coefficient ($q = d\lambda/dH_{DC}$) of Metglas is positive ($+q$), opposite to that of Ni ($-q$), a bending actuation of the Metglas/PZT/Ni laminate beam can be promoted when exposed to H_{AC} [15]. This approach was effective for achieving low frequency bending resonance of the laminate as shown in Fig. 1d. The Metglas/PZT/Ni laminate without Nd magnets exhibited a bending resonance peak at 483 Hz. The bending resonance peak was further reduced to around 260 Hz by attaching the Nd tip masses, regardless of the attachment layout. The structural bending characteristic is clearly identified by the actuation shape of the Metglas/PZT/Ni laminate in Fig. 1e.

Figure 2 shows the ME voltage coefficient ($\alpha_{ME} = E_{AC}/H_{AC}$, E_{AC} : output electric field) versus H_{DC} curves of the Metglas/PZT/Ni laminate for the magnet attachment layouts (i) and (ii) shown in Fig. 1b. For the layout (i), we investigated two cases: Nd magnets on Metglas surface (case 1) and Nd magnets on Ni surface (case 2). As can be seen in Fig. 2a, the α_{ME} versus H_{DC} curves in both cases deviate significantly from the symmetrical shape for both H_{DC} and α_{ME} axes (unlike the symmetrical curve of the laminate without Nd magnets in Fig. 1f), exhibiting giant

α_{ME} - values at $H_{DC} = 0$ (α_{SME}). The amount shifted on the H_{DC} axis from the origin (ΔH) is determined by the H_{PA} distribution inside the MS layers. The ΔH indicates the H_{DC} required to zero the effective magnetization in the MS layers. In addition, the integral of α_{ME} over H_{DC} reflects the effective λ (λ_{eff}) of the MS layer (Fig. 2b) since the α_{ME} is directly proportional to the q [16]. In case 1, the ΔH and resultant α_{SME} were 20.42 Oe and $52.35 \text{ V cm}^{-1} \text{ Oe}^{-1}$, respectively. In case 2, the ΔH was 13.51 Oe and the observed α_{SME} value ($23.39 \text{ V cm}^{-1} \text{ Oe}^{-1}$) was less than half of case 1. Interestingly, in case 1, the amount of α_{ME} of increasing-field maximum ($+\alpha_{MAX}$) (point a) was larger than that of decreasing-field maximum ($-\alpha_{MAX}$) (point b), whereas in case 2, $+\alpha_{MAX}$ (point c) was smaller than $-\alpha_{MAX}$ (point d). However, for the layout (ii), there was no significant difference between $+\alpha_{MAX}$ and $-\alpha_{MAX}$ values as shown in Fig. 2c. The ΔH and α_{SME} for the layout (ii) were 20.97 Oe and $28.25 \text{ V cm}^{-1} \text{ Oe}^{-1}$, respectively.

To elucidate the differences between the α_{ME} versus H_{DC} curves observed in layouts (i) and (ii), we considered the distribution of the magnetic field due to Nd magnets as shown in Fig. 2d. For the layout (i), the H_{PA} is concentrated on the upper MS layer and relatively weak inside the lower MS layer when $H_{DC} = 0$. Moreover, a non-negligible outside

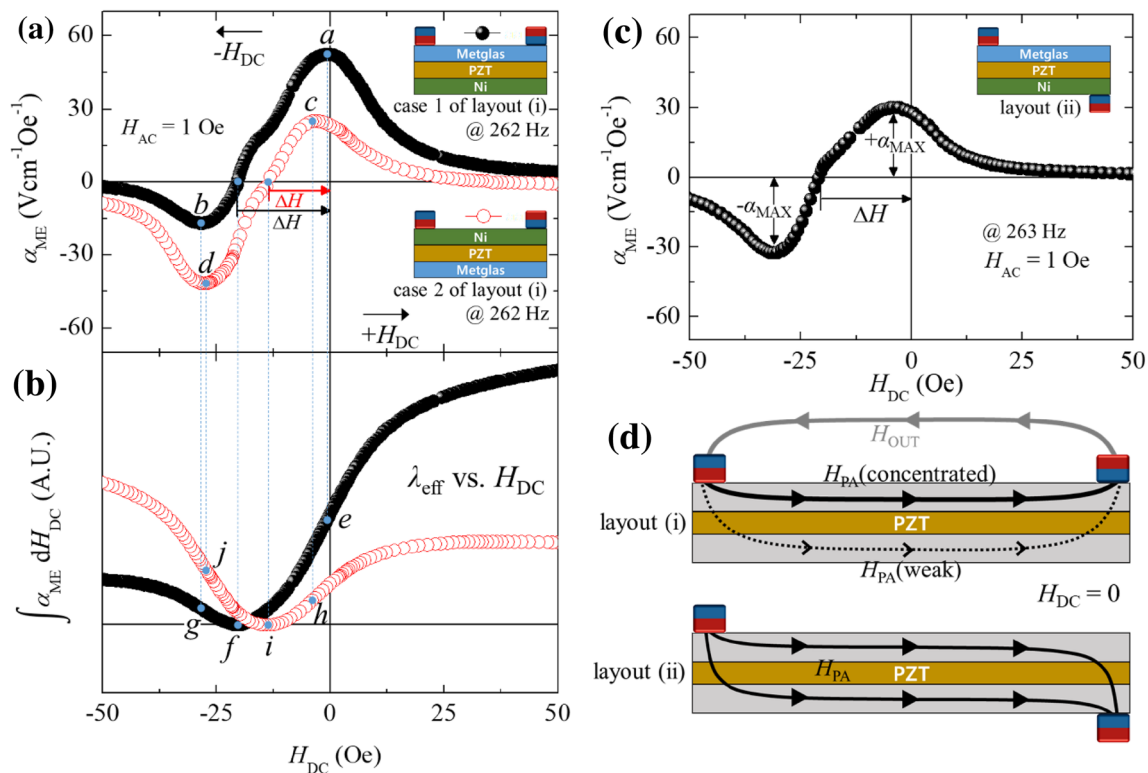


Fig. 2 a α_{ME} versus H_{DC} curves of Metglas/PZT/Ni laminates with layout (i) measured under H_{AC} of 1 Oe at bending resonance frequencies. b Integral values of α_{ME} with respect to H_{DC} for layout (i). c α_{ME} versus H_{DC} curve of Metglas/PZT/Ni laminate with layout (ii) measured

under H_{AC} of 1 Oe at bending resonance frequency. d Schematics of magnetic field formation by a pair of Nd magnets for layouts (i) and (ii). (Color figure online)

magnetic field (H_{OUT}) exists above the laminate between two Nd magnets. In this situation, we first analyze the change in α_{ME} under the H_{DC} applied in reverse direction ($-\overline{H_{DC}}$) for the case 1 (from point a to point b) and case 2 (from point c to point d) in Fig. 2a. In case 1, the $+\alpha_{MAX}$ appears near $H_{DC}=0$ (point a), implying that the slope of λ_{eff} curve (i.e., q) of the MS layers is maximized by the H_{PA} (point e). As the $|\overline{H_{DC}}|$ increases gradually by ΔH , the slope of λ_{eff} curve gradually decreases and becomes zero at point f . Here, the effective strain of Metglas and Ni layers is zero under $H_{AC}=1$ Oe, i.e., the direction of local magnetic dipoles in those MS layers is nominally random. After then, the local magnetic dipoles start to align in the direction of the $-\overline{H_{DC}}$ with further increasing the field strength, and the second maximum of the slope of λ_{eff} curve appears at point g , resulting in the $-\alpha_{MAX}$ (point b). Note that during the progression from point a to point b , the directions of H_{OUT} and $-\overline{H_{DC}}$ coincide with each other. Then, a significant amount of attraction force by the H_{OUT} causes compressive stress on Metglas layer and tensile stress on Ni layer. Both of these stresses are contrary to the piezomagnetic nature of Metglas ($+q$) and Ni ($-q$), therefore, the $-\alpha_{MAX}$ should be smaller than the $+\alpha_{MAX}$.

For the case 2, the $+\alpha_{MAX}$ appears at point c (maximum slope of λ_{eff} curve at point h), implying that the H_{PA} is slightly larger than the amount needed to obtain the maximum α_{SME} . Moreover, the ΔH , the amount of $-\overline{H_{DC}}$ required to zero the slope of λ_{eff} curve (point i), is smaller than that of case 1. These are possibly owing to the difference in λ versus H_{DC} characteristics between Metglas and Ni. For the layout (i), since the H_{PA} is concentrated in the MS layer with Nd magnets, it is natural to consider that the upper MS layer dominates the initial ME response. For the case 1 of layout (i), the concentrated H_{PA} is appropriate to obtain the highest slope of λ versus H_{DC} curve of Metglas, thus, the α_{SME} is almost identical to the $+\alpha_{MAX}$. Meanwhile, for Ni, the maximum q value and the H_{DC} value required for the maximum q are all smaller than those of Metglas [17]. Therefore, for the case 2, the ΔH should be smaller than that of case 1, and the α_{SME} is smaller than the $+\alpha_{MAX}$. The difference in $+\alpha_{MAX}$ value between cases 1 and 2 demonstrates well that the upper MS layer dominates the ME response for the layout (i). Next, we again invoke the presence of H_{OUT} for the larger $-\alpha_{MAX}$ (point d) than the $+\alpha_{MAX}$ (point c) in case 2. For the case 2, the upper Ni layer experiences compressive stress by the H_{OUT} while the lower Metglas layer is under tensile stress during the reverse biasing ($-\overline{H_{DC}}$). In this case, these stresses correspond to the bending motion of the laminate due to the piezomagnetic nature of Metglas ($+q$) and Ni ($-q$), resulting in the highest slope of λ_{eff} curve at point j . However, for the layout (ii) in Fig. 2d, the H_{PA} is evenly distributed in the upper and lower MS layers and the

H_{OUT} between two Nd magnets is negligible. Therefore, the magnitude of $+\alpha_{MAX}$ is very similar with that of $-\alpha_{MAX}$ due to the absence of stresses causing bending motions as shown in Fig. 2c. Furthermore, both $+\alpha_{MAX}$ and α_{SME} values of the laminate with layout (ii) were found to be smaller than those of case 1 and larger than those of case 2 of layout (i), demonstrating the concurrent contribution of Metglas and Ni layers to the initial ME response for the layout (ii). From the above results, one can find that the laminate structure in which the H_{PA} is concentrated in Metglas layer is effective in obtaining a high α_{SME} .

Figure 3a shows the α_{ME} versus H_{DC} curves of the Metglas/PZT/Ni laminate for the magnet attachment layouts (iii) and (iv) in Fig. 1b. For the layout (iii), although the H_{PA} is expected to be concentrated in the Metglas layer as shown in Fig. 3b, its $+\alpha_{MAX}$ ($18.04 \text{ V cm}^{-1} \text{ Oe}^{-1}$) was much smaller than that of the case 1 of layout (i). Moreover, the ΔH was 35.63 Oe, which is almost 70% larger than that of the case 1 of layout (i), and resultant α_{SME} was also relatively low ($14.11 \text{ V cm}^{-1} \text{ Oe}^{-1}$). In the case of layout (iv), both $+\alpha_{MAX}$ and α_{SME} values were found to be slightly larger than those of the layout (iii), implying that the Metglas layer with

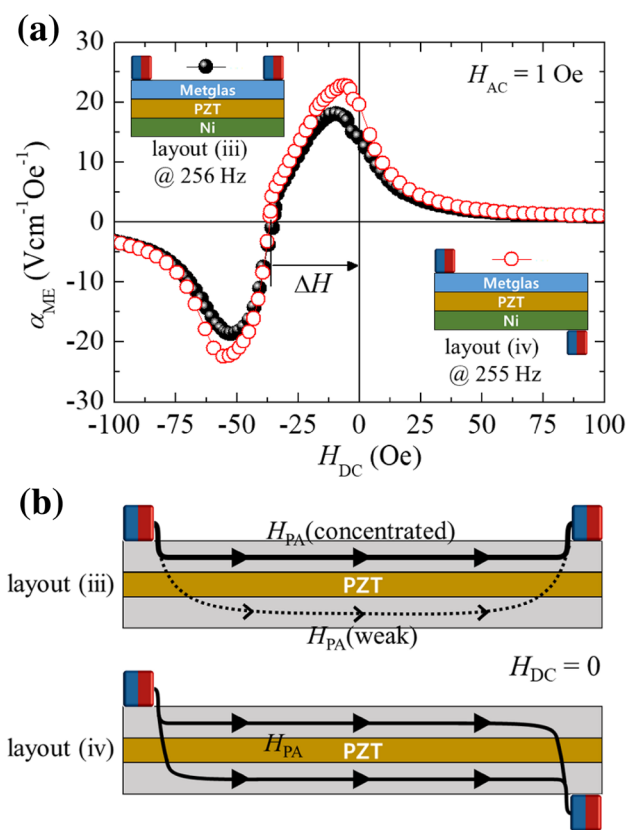


Fig. 3 **a** α_{ME} versus H_{DC} curves of Metglas/PZT/Ni laminates with layouts (iii) and (iv) measured under H_{AC} of 1 Oe at bending resonance frequencies. **b** Schematics of magnetic field formation by a pair of Nd magnets for layouts (iii) and (iv). (Color figure online)

concentrated H_{PA} did not dominate the ME response in layout (iii). For both layout (iii) and layout (iv), the magnitude of $+\alpha_{MAX}$ was similar to that of $-\alpha_{MAX}$ due to the absence of an influenceable H_{OUT} (Fig. 3b). The α_{ME} versus H_{DC} curve of the laminate with layout (iv) looks very similar to that of the laminate with layout (ii) in Fig. 2c, however, the ΔH and α_{SME} of layout (iv) are quite different from those of layout (ii) despite their similar structures.

The α_{SME} values of layouts (iii) and (iv) are smaller than those of layouts (i) (case 1) and (ii), therefore, it can be recognized that the change in λ of the MS layer ($\Delta\lambda$) under a H_{AC} at $H_{DC}=0$ is larger in $\overline{M}_{Nd}(\perp)$ case rather than in $\overline{M}_{Nd}(\parallel)$ case. To understand the underlying mechanism of the phenomena found, we considered in more detail the distribution of H_{PA} by Nd magnets and the resultant magnetization distributions inside the MS layer for both cases as shown in Fig. 4. The H_{PA} by Nd magnets aligns the local magnetizations (or magnetic dipole moments in local domains) in MS layer ($\delta\overline{M}_{MS}$). Schematics of the expected distribution of H_{PA} and $\delta\overline{M}_{MS}$ are shown in Fig. 4a, b for the $\overline{M}_{Nd}(\perp)$ and $\overline{M}_{Nd}(\parallel)$ cases, respectively. Due to the difference in layout of attaching Nd magnets, the H_{PA} and resultant $\delta\overline{M}_{MS}$ distribution shows a difference between $\overline{M}_{Nd}(\perp)$ and $\overline{M}_{Nd}(\parallel)$ cases. Based on the expected H_{PA} distribution, we figured out two

different magnetization regions in the MS layer (regions I and II) as shown in Fig. 4. In region I, all magnetic domains are parallel to the longitudinal direction, whereas in region II, the direction of the magnetic domains is not parallel to the longitudinal direction. In both $\overline{M}_{Nd}(\perp)$ and $\overline{M}_{Nd}(\parallel)$ cases, the strength of H_{PA} is high enough to saturate the $\delta\overline{M}_{MS}$ magnitude adjacent to the Nd magnet and lowest at the center of the laminate, resulting in a gradient of $\delta\overline{M}_{MS}$ magnitude across the MS layer. For the $\overline{M}_{Nd}(\perp)$ case, region I consists of magnetic domains with small $\delta\overline{M}_{MS}$ magnitudes parallel to the longitudinal direction, and region II consists of magnetic domains with various angles (θ_i) to the longitudinal direction and almost saturated $\delta\overline{M}_{MS}$ magnitude. However, for $\overline{M}_{Nd}(\parallel)$ case, region I is wider than that of $\overline{M}_{Nd}(\perp)$ case and consists of magnetic domains with various $\delta\overline{M}_{MS}$ magnitudes ranging from a small value to a saturation value. The region II of $\overline{M}_{Nd}(\parallel)$ case is much narrower than that of $\overline{M}_{Nd}(\perp)$ case, and magnetic domains with $\theta_i=90^\circ$ and 180° are expected to dominate in this region.

For detailed analysis of the $\Delta\lambda$ due to the redistribution of $\delta\overline{M}_{MS}$ under small fluctuations of H_{DC} (δH_{DC} : amplitude of H_{AC}) in regions I and II, we considered the contribution of $\Delta\lambda$ owing to the change in the magnitude of $\delta\overline{M}_{MS}$ ($\Delta\lambda(M)$) and the contribution of $\Delta\lambda$ owing to the rotation of $\delta\overline{M}_{MS}$

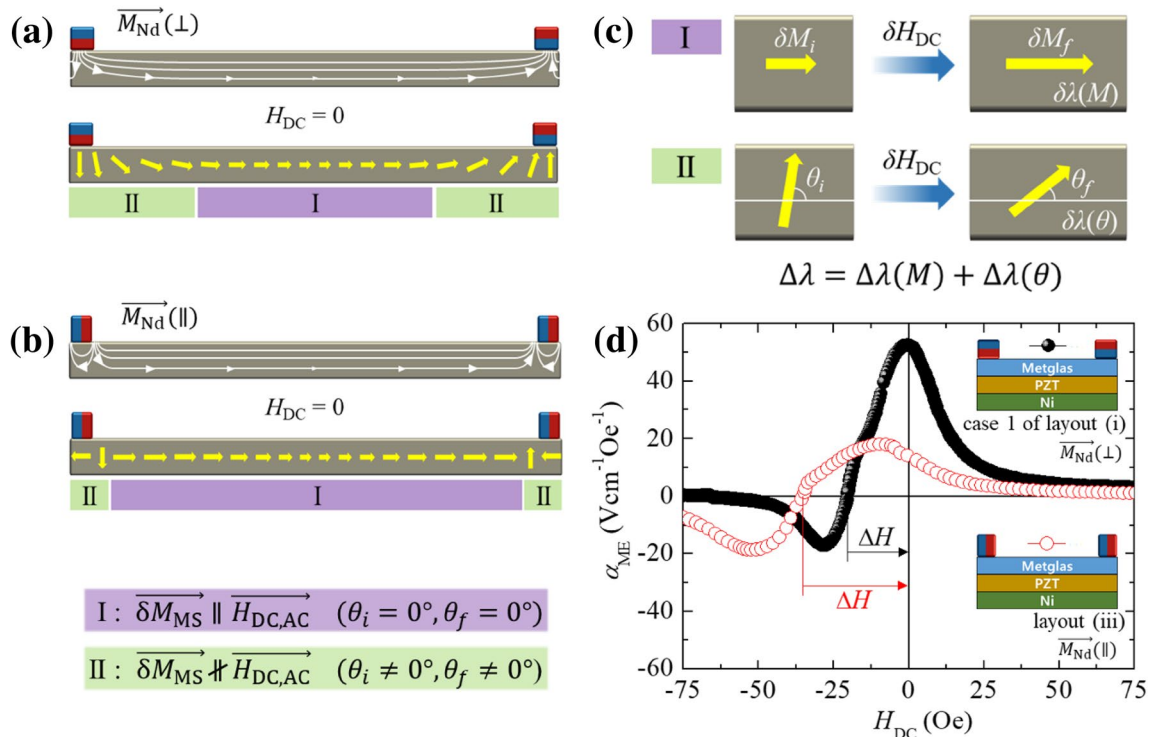


Fig. 4 Schematics of distribution of H_{PA} (white lines) and $\delta\overline{M}_{MS}$ (yellow arrows) in MS layer when $H_{DC}=0$: **a** \overline{M}_{Nd} is perpendicular, and **b** \overline{M}_{Nd} is parallel to the longitudinal direction of the laminate. The size of arrow head on white line reflects the strength of H_{PA} . The length of yellow arrows indicates the magnitude of $\delta\overline{M}_{MS}$. **c** Schematics

of $\Delta\lambda(M)$ and $\Delta\lambda(\theta)$ contribution to total $\Delta\lambda$ when $H_{DC}\neq 0$. **d** α_{ME} versus H_{DC} curves of Metglas/PZT/Ni laminates with layouts (i) and (iii) measured under H_{AC} of 1 Oe at bending resonance frequencies. (Color figure online)

($\Delta\lambda(\theta)$) as shown in Fig. 4c. The $\Delta\lambda(M)$ is determined by the following relation [18]:

$$\lambda = \frac{3\lambda_S}{2M_S^2} M^2, \quad (1)$$

where λ_S is a saturated magnetostriction and M_S is a saturated magnetization. The $\Delta\lambda(\theta)$ is expressed by [18]:

$$\Delta\lambda(\theta) = \frac{3\lambda_S}{2} [\langle \cos^2 \theta_f \rangle - \langle \cos^2 \theta_i \rangle], \quad (2)$$

where the angular brackets represent an average of $\cos^2\theta$ over all orientations in the initial state (θ_i) and the final state (θ_f). In region I, the $\Delta\lambda(\theta)$ is negligible ($\theta_i \approx \theta_f$) and the $\Delta\lambda(M)$ can be regarded similar for both $\overline{M_{Nd}(\perp)}$ and $\overline{M_{Nd}(\parallel)}$ cases because only unsaturated $\delta\overline{M_{MS}}$ in region I contribute to the $\Delta\lambda(M)$. However, the $\Delta\lambda(\theta)$ in region II of $\overline{M_{Nd}(\perp)}$ case is non-negligible and effectively contribute to total $\Delta\lambda$. Although the $\Delta\lambda(\theta)$ in region II of $\overline{M_{Nd}(\parallel)}$ case is not zero, its contribution to total $\Delta\lambda$ is very small due to the narrow region having magnetic domains with $\theta_i = 90^\circ$. The magnetic domains with $\theta_i = 180^\circ$ in region II of $\overline{M_{Nd}(\parallel)}$ case are hardly believed to contribute to total $\Delta\lambda$ because the sign of $\Delta\lambda(M)$ in this case is opposite. Therefore, a larger $\Delta\lambda$ and a higher α_{SME} can be obtained in $\overline{M_{Nd}(\perp)}$ case rather than in $\overline{M_{Nd}(\parallel)}$ case under the same δH_{DC} (or H_{AC}). Furthermore, comparing Fig. 4a, b, it is clear that the magnitude of the magnetization parallel to the longitudinal direction of the laminate (i.e. parallel to the H_{DC}) in region I is much smaller in $\overline{M_{Nd}(\perp)}$ case than in $\overline{M_{Nd}(\parallel)}$ case. This implies that the H_{PA} parallel to the H_{DC} is larger in $\overline{M_{Nd}(\parallel)}$ case, therefore, the ΔH should also be larger in $\overline{M_{Nd}(\parallel)}$ case as shown in Fig. 4d.

Finally, we note that the α_{SME} value (or SME voltage output) can be easily adjusted in our device structures, by simply changing the direction of magnetic tip masses. We believe this advantage will impose ease on the fabrication of tunable SME devices.

3 Conclusions

In conclusion, strong SME responses were experimentally verified for the Metglas/PZT/Ni laminate structures with magnetic tip masses. Based on detailed analysis of ME characteristics of the laminates with four different layouts of attaching two permanent magnets, we demonstrated that the highest SME effect could be obtained when both magnetic tip masses are loaded on Metglas layer (high + q material) and their magnetization direction is normal to the Metglas surface. Identifying the cause of the observed ME responses, we proposed that non-parallel ferromagnetic dipoles contribute to the total magnetostriction effectively without affecting the amount of ΔH . The pre-biased Metglas/PZT/Ni laminate

exhibited giant SME voltage coefficients ranging from 14.11 to 52.35 V cm⁻¹ Oe⁻¹ at around 260 Hz under 1 Oe, demonstrating its implementation potential for precision field sensors, magnetic energy harvesters, and field-tunable SME devices as well.

Acknowledgements This work was supported by the Fundamental Research Program of the Korea Institute of Materials Science (KIMS) (Grant No. PNK6030), the National Research Foundation (NRF) of Korea funded by the Ministry of Education [Grant No. NRF-2019R111A3A01058105] and [NRF-2018R1A6A1A03025761].

References

- Palneedi, H., Maurya, D., Geng, L.D., Song, H.-C., Hwang, G.-T., Peddigari, M., Annapureddy, V., Song, K., Oh, Y.S., Yang, S.-C., Wang, Y.U., Priya, S., Ryu, J.: Enhanced self-biased magnetoelectric coupling in laser-annealed Pb(Zr, Ti)_{0.3} thick film deposited on Ni foil. *ACS Appl. Mater. Interfaces* **10**(13), 11018–11025 (2018)
- Nan, C.-W., Bichurin, M.I., Dong, S., Viehland, D., Srinivasan, G.: Multiferroic magnetoelectric composites: historical perspective, status, and future directions. *J. Appl. Phys.* **103**, 031101–0311035 (2008)
- Palneedi, H., Annapureddy, V., Priya, S., Ryu, J.: Status and perspectives of multiferroic magnetoelectric composite materials and applications. *Actuators* **5**, 9 (2016)
- Lage, E., Kirchhof, C., Hrkac, V., Kienle, L., Jahns, R., Knöchel, R., Quandt, E., Meyners, D.: Exchange biasing of magnetoelectric composites. *Nat. Mater.* **11**, 523–529 (2012)
- Fiebig, M.: Revival of the magnetoelectric effect. *J. Phys. D: Appl. Phys.* **38**, R123–R152 (2005)
- Ryu, J., Carazo, A.V., Uchino, K., Kim, H.-E.: Magnetoelectric properties in piezoelectric and magnetostrictive laminate composites. *Jpn. J. Appl. Phys.* **40**, 4948–4951 (2001)
- Chen, L., Li, P., Wen, Y., Zhu, Y.: Large self-biased effect and dual-peak magnetoelectric effect in different three-phase magnetostrictive/piezoelectric composites. *J. Alloys. Compd.* **606**, 15–20 (2014)
- Hwang, G.-T., Palneedi, H., Jung, B.M., Kwon, S.J., Peddigari, M., Min, Y., Kim, J.-W., Ahn, C.-W., Choi, J.-J., Hahn, B.-D., Choi, J.-H., Yoon, W.-H., Park, D.-S., Lee, S.-B., Choe, Y., Kim, K.-H., Ryu, J.: Enhancement of magnetoelectric conversion achieved by optimization of interfacial adhesion layer in laminate composites. *ACS Appl. Mater. Interfaces* **10**(38), 32323–32330 (2018)
- Zhou, Y., Maurya, D., Yan, Y., Srinivasan, G., Quandt, E., Priya, S.: Self-biased magnetoelectric composites: an overview and future perspectives. *Energy Harvest. Syst.* **3**, 1–42 (2016)
- Li, M., Wang, Z., Wang, Y., Li, J., Viehland, D.: Giant magnetoelectric effect in self-biased laminates under zero magnetic field. *Appl. Phys. Lett.* **102**(8), 082404 (2013)
- Nogués, J., Schuller, I.K.: Exchange bias. *J. Magn. Magn. Mater.* **192**(2), 203–232 (1999)
- Deka, B., Ravi, S., Perumal, A.: Study of exchange bias in Mn-doped YFeO₃ compound. *J. Supercond. Nov. Magn.* **29**(8), 2165–2170 (2016)
- Martin, L.W., Crane, S.P., Chu, Y.H., Holcomb, M.B., Gajek, M., Huijben, M., Yang, C.H., Balke, N., Ramesh, R.: Multiferroics and magnetoelectrics: thin films and nanostructures. *J. Phys.: Condens. Matter* **20**(43), 434220 (2008)

14. Vaz, C.A.F., Hoffman, J., Ahn, C.H., Ramesh, R.: Magnetolectric coupling effects in multiferroic complex oxide composite structures. *Adv. Mater.* **22**(26–27), 2900–2918 (2010)
15. Yoo, I.-R., Ahn, C.-W., Cho, K.-H.: 15-Mode piezoelectric composite and its application in a magnetolectric laminate structure. *J. Alloy. Compd.* **767**, 61–67 (2018)
16. Yang, S.C., Cho, K.-H., Park, C.-S., Priya, S.: Self-biased converse magnetolectric effect. *Appl. Phys. Lett.* **99**(20), 202904 (2011)
17. Zhou, Y., Yang, S.C., Apo, D.J., Maurya, D., Priya, S.: Tunable self-biased magnetolectric response in homogenous laminates. *Appl. Phys. Lett.* **101**(23), 232905 (2012)
18. Cullity, B.D., Geraham, C.D.: *Introduction to Magnetic Materials*. Wiley, Hoboken (2009)

Publisher's Note Springer Nature remains neutral with regard to jurisdictional claims in published maps and institutional affiliations.